

# Photometric treatment of HD100453

Semester Project

Ulrich Sauter

Supervisor: Prof. Dr. Hans Martin Schmid

Co-Supervisor: Jie Ma

Department of Physics

ETH Zürich

June, 2020

## Abstract

The cyc116 observation has a saturated central star. To fix this, the azimuthal average profile of the ND4 observations was fitted to that of cyc116. With the fixed peak, aperture photometry was used to determine the stellar magnitudes of the objects in cyc116. The radial Stokes parameter  $Q_\phi$  was used as well as an estimate of the disk flux to determine the color of the protoplanetary disk of HD 10453.

## 1 Introduction

### 1.1 Observations

The object of interest in this project is the HD 100453 system. It consists of the central star HD 100453 A, which is a Herbig Ae/Be Star with a protoplanetary disk located in the Lower Centaurus Association. HD 100453 A has also an early-M star companion, called HD 100453 B. A distant star is located to the top left of HD 100453 A. There are also two ghosts from the central star visible. A ghost gets produced by the reflection of light at both sides of the telescope lens. The speciality of the HD 100453 system comes from the protoplanetary disk that is around HD 100453 A. The light scattered from the disk gets polarized, while the light coming directly from the central star is unpolarized. The observations used in this project were all taken from the ZIMBOL imager at ESO's Very Large Telescope (VLT) in Chile. An observation has 4 frames corresponding to the 4 Stokes parameters.

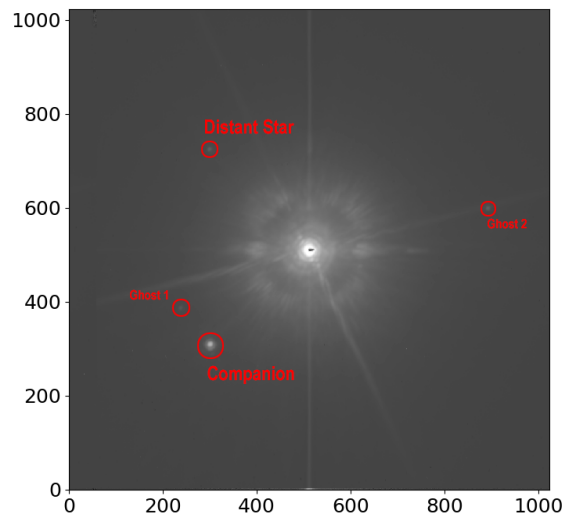


Fig. 1  $I_Q$  frame in the I-band of cyc116 in logarithmic scale.

One set of observations is called cyc116 and it consists of an observation with the R\_PRIM filter, central wavelength 626.3 nm, and another with the I\_PRIM filter, central wavelength of 789.7 nm. Looking at the  $I_Q$  frame of cyc116 in figure 1, we see that the observation is bad. The central star is saturated, recognizable by the black dot inside the star. This is the case for all observation of the cyc116 set. Due to this a correct flux measurement of the central star is not possible but the observation is still useful to measure the disk and the other objects.

To solve the issue of cyc116, we have another set of observations, the ND4 set. The ND4 observations and cyc116 were taken just a few minutes apart, so the environmental condition should be similar. The difference between them is that an additional neutral density filter (ND4) was applied for the ND4 observations. The neutral density filter reduced the counted photons on average by a factor of  $10^{-4}$  (see figure 2), depending on the wavelength of light. We have as well one observation with the I\_PRIM filter and the R\_PRIM filter. The objective is to match the ND4 observation to the one of cyc116 to reconstruct the peak of HD 100453 A.

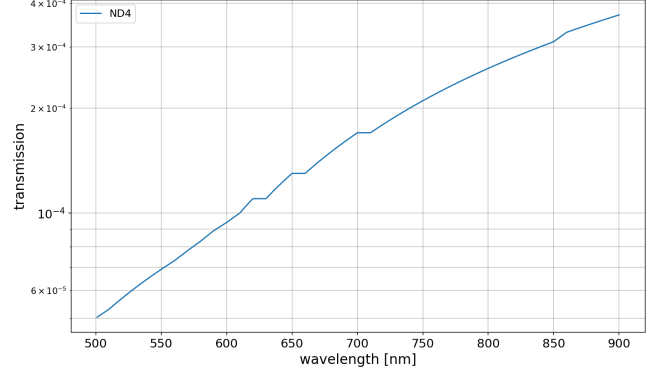


Fig. 2 ND4 filter transmission coefficient.

We used another set of observations called point spread function (PSF). The PSF describes how a point source of light is spread over the detected image. With the PSF we can estimate the flux of the central star, without any additional scattered light from the disk.

The radial stokes parameter is given by

$$Q_\phi = -Q \cos 2\phi + U \sin 2\phi,$$

with  $\phi$  being the position angle of the location  $(x, y)$  with respect to HD 100453 A at  $(x_0, y_0)$  and is written as  $\phi = \arctan \frac{x-x_0}{y-y_0}$ . For more information see [1]. With  $Q_\phi$ , we can show the scattered light from the disk as positive flux.

The second objective is to calculate the stellar magnitude of the objects visible in cyc116.

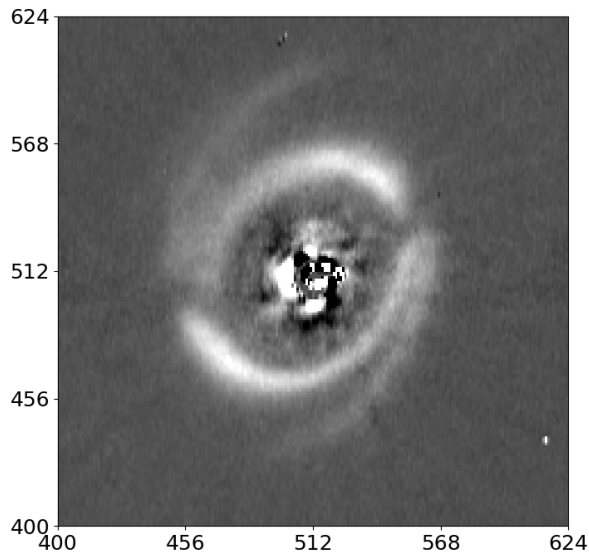


Fig. 3 Zoomed in picture of the radial polarization  $Q_\phi$  of cyc116 in the I-band. We see the disk as well as two spiral caused by the orbit of the companion.

## 1.2 Methods

### 1.2.1 Aperture Photometry

Aperture photometry is the simplest method to obtain a flux measurement  $\Phi$  of an object. It is done by integrating all the values within a circular aperture centered on the object, marked orange in figure 4, to get a total value. After that, the background level needs to be subtracted. The normal way to do this is to calculate the median of the background in an annulus around the aperture, marked red and then subtracting this median multiplied by the number of pixels in the aperture from the total value. Another way we tried to subtract the background level is by fitting a second order polynomial to the background. The final flux was then obtained by subtracting the polynomial from the aperture. We will compare these two methods in section 2.2.1 to see if the extra effort was worth it.

Once all the fluxes are calculated, we can calculate the color magnitude of the objects by using the fluxes in the I and R-band

$$\Delta m = -2.5 \log \frac{\Phi_I}{\Phi_R} = m_I - m_R. \quad (1.1)$$

With the color magnitude, one can estimate the temperature of a star. The same formula 1.1 can also be used to calculate the magnitude difference between two objects. We can apply the same procedure with a slight modification to the disk of HD 100453 A. Instead of using a circular aperture, we replace it with an annular aperture to ignore the flux produced by the star.

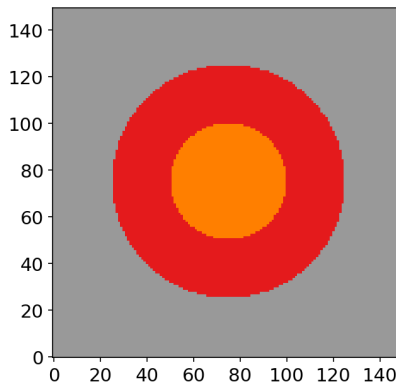


Fig. 4 Example aperture with an orange aperture and red annulus.

### 1.2.2 Azimuthal averaged profile

An azimuthal averaged profile, hereafter referred to as profile, is created by averaging over all points, which have the same distance from the center of the image. This makes for an appropriate data reduction method to simplify the data to 1 dimension because we expect that the emission of the star is radial symmetric.

## 2 Data analysis

### 2.1 Isolating the disk

We worked with the profiles of the observations because it allowed us to simplify the fitting process to one dimension. First, we needed to reconstruct the peak of the cyc116 profile. For

that, the profile of the ND4 observation needed to be rescaled to fit that of cyc116. The profile thus obtained was called the scaled profile. After this, we needed to remove the emission from the star to get the disk flux. To accomplish this, the PSF profile was fitted to the peak of the scaled profile, resulting in a profile called star profile.

### 2.1.1 Rescaling of the ND4 profile

A simple multiplication with just a scaling factor didn't work. The reason was, that the ND4 profile is reduced by a factor of  $\sim 10^{-4}$ . So the background will also get amplified by the same factor during the rescaling. This led to unwanted results because of the high background level. To prevent this from happening, it was necessary to first subtract a constant from the profile to reduce the background level. This resulted in the following fitting function:

$$f_1(x, a, b) = a \cdot (x - b) \quad (2.1)$$

Since we were mostly interested in the reconstruction of the peak, we needed to adjust the fitting region accordingly. We excluded the first 14 data points to avoid the effect of the over saturation and also excluded the points outside a radius of 65 px. We obtained a good estimate of the starting values by calculating the inverse transmission factor of the neutral density filter for  $a$  and by taking the median of the background for  $b$ . The fitting method yielded parameters close to our estimate, which means we correctly assumed the meaning of the fitting parameters.

### 2.1.2 Fitting of the PSF

Next, we fitted the PSF profile to the scaled profile. We adopted the method above with slight changes to the fitting region. Instead of the interval, we used the first 32px. We only used the pixels at the peak, because the PSF profile and scaled profile had a difference further away from the peak. The difference is due to the reflected light from the disk. The resulting fit matched the peak well, but the background dropped off too quickly, see figure 5. To counteract this behaviour we increased the fitting region by including 5 points between 120px-200px ("tail") to control the residue of the background. To also make up for the fewer points inside the tail, the weight of those points got increased.

The fitting routine still performed poorly, due to the amplified noise of the scaled profile in the outer region. The difficulty was to choose good points for tail near the cyc116 profile. To achieve this, we tried in a first attempt to only choose points within a  $\sigma$  interval of the cyc116 profile. But still, this method resulted often in errors because, for some configuration of parameters, no points were close to the cyc116 profile. We settled for a much simpler method, by creating a new mixed profile. The idea was to combine the peak of the scaled profile and use the cyc116 profile for the rest. We compared the two profiles to find a good transition point for creating the mixed profile.

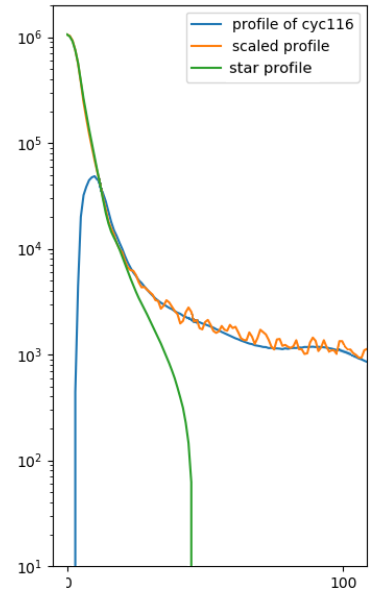


Fig. 5 Fit (green) with no additional points in tail.

### 2.1.3 Comparison

To compare the two profiles, we divided the cyc116 profile by the scaled profile. The result is shown in figure 6. We see that for the first 20px the difference of the two profiles is within  $\pm 10\%$ . This makes for a good transition point for the mixed profile. We chose the transition to be at pixel 21. Therefore the mixed profile consisted of the first 21px of the scaled profile while the rest was the cyc116 profile. This assured us that we have a correct fit of the peak while having good control over the background level.

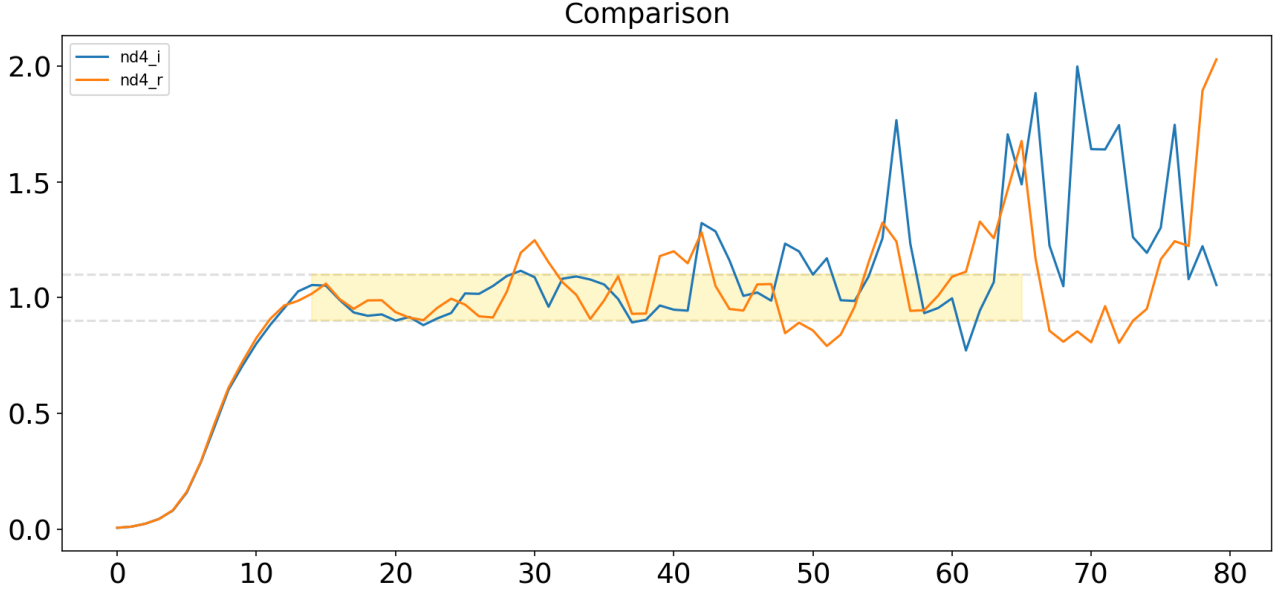


Fig. 6 The cyc116 profile divided by the scaled profile. The yellow marked region is the fitting area. The dashed lines are positioned at distance of 0.1 away from 1.

### 2.1.4 Fitting with the mixed profile

Finally, to improve the fit of the PSF and adding an additional degree of freedom, we added a convolution with a Gaussian of standard deviation  $\sigma$  to the fitting method. Resulting in the fitting function:

$$f_2(x, a, b, \sigma) = a \cdot (\text{gauss}(x, \sigma) - b) \quad (2.2)$$

All the profiles are shown in figure 7. The results looked good but there were still some problems. One problem is that the fitted PSF profile got sometimes over and sometimes under the profile of cyc116. This results in positive and negative values when we did the subtraction, more on that in the next section.

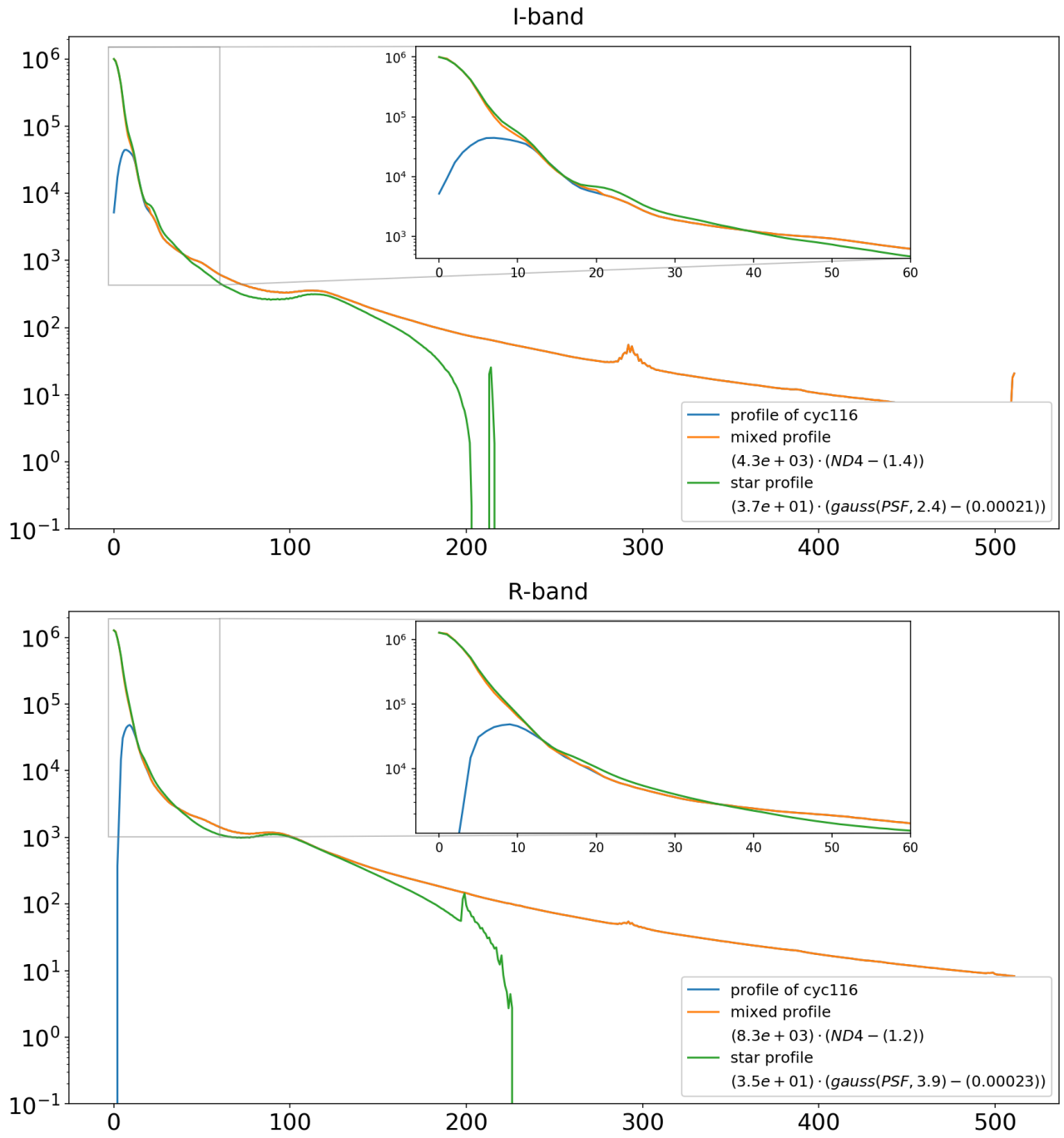


Fig. 7

### 2.1.5 Isolating disk

For a first estimate of the disk flux, we can subtract the mixed profile and star profile resulting in figure 8.

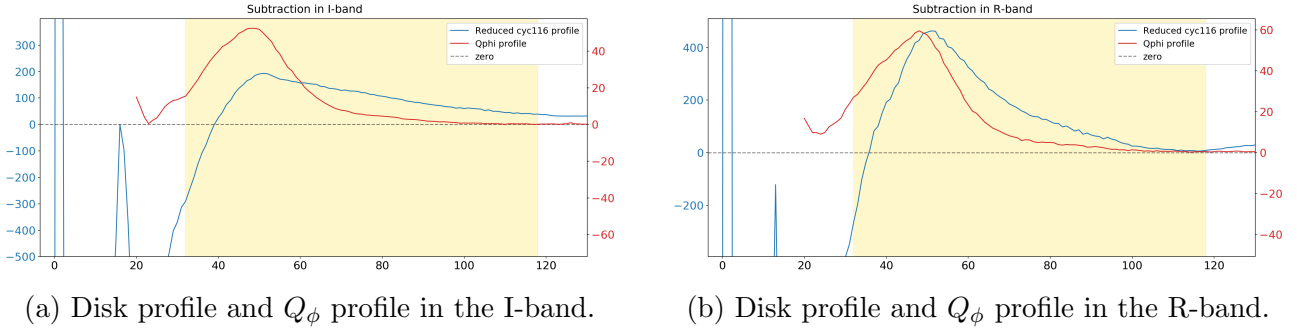


Fig. 8 The cyc116 profile subtracted by the star profile (blue) and the profile of  $Q_\phi$  (red). The points inside the yellow region were used to estimate the flux of the disk. Scale on the left for the blue line and scale on the right for the red.

We can see a peak around 50px, which corresponds to our disk. This is further validated by the  $Q_\phi$  profile. We also see some problems with the fit. We have positive and negative values in the first few pixels and can't determine where the disk starts. We also have a discrepancy of the values outside of the cyc116 profile and the star profile. Which leads to an increase of the subtracted profile further out.

To get a first estimate of the disk flux, we integrated the values inside the yellow region. The yellow region stretches from 28px to 93px. This is the same size as the aperture used to calculate the disk flux in table 6. The results of the  $Q_\phi$  profile should be slightly bigger than that in the table because we didn't subtract the background level.

By investigating how much light gets scattered by disk in the different wavebands, we can make a prediction on the density of the material in the disk. By dividing the flux of the disk by the flux of the central star, we get . The results are shown in table 2. We see that for both estimates of the disk flux the I-band value is bigger. This suggest a reddish color for the disk, meaning the material in the disk is grainy.

	I-band	R-band
Disk profile	$3.64 \cdot 10^6$	$5.17 \cdot 10^6$
$Q_\phi$ profile	$4.37 \cdot 10^5$	$4.92 \cdot 10^5$

Table 1: Calculated fluxes for the Disk and  $Q_\phi$ .

	I-band	R-band
Disk profile	2.7%	2.4%
$Q_\phi$	0.31%	0.22%

Table 2: Ratio between the disk,  $Q_\phi$  flux and the mixed profile flux. We used the numbers in table 3 for  $Q_\phi$ .

## 2.2 Photometric Analysis

A complete and accurate analysis requires a not to faint observation and one without a saturated object. To make a photometric analysis we did the following steps:

1. The flux of a big aperture centered around the central object needs to be calculated. We chose a radius of 417px which corresponds to  $3''$ .
2. Find the stellar magnitude of the central object from literature. In our case, it is 7.42 mag in the I-band and 7.6 mag in the R-band (table 2 of [2]).
3. Not all objects can be measured in the big apertures, therefore, we need to introduce small apertures around every object of interest. To get comparable results between the objects, it is important to choose the same aperture for every object. We chose a radius of 20px for the small aperture.
4. We can associate the flux from step 1. to a stellar magnitude. To determine the magnitude of the other objects, we can calculate the flux ratio to the central object and use equation (1.1). The general rule is, if an object has 10 times less flux, it has a 2.5 higher magnitude.

### 2.2.1 Background removal

To compare the two background removal methods, we will apply them on the companion and ghost 2. These objects were chosen because the surrounding of the companion is simple and the surrounding of the ghost is complex as a consequence of the spider.

For the first method in the I-band  $I_Q$ -frame, the flux is written in table 6. The same size of aperture with the second method results in a flux with removed background of  $3.90 \cdot 10^5$  for the companion and  $1.65 \cdot 10^4$  for the ghost. If we assume the measurement error is given by the difference of the  $I_Q$  and  $I_U$  values, the fluxes of the second method are not significantly different. We can conclude, that it is better to just use the first, simpler method.

### 2.2.2 Magnitudes

Since we have the saturation problem in the cyc116 observation, we can't use it for the complete analysis. Fortunately, we made in the previous section the mixed profile, which should be identical to the cyc116 observation but without the saturation. We can check if the mixed profile makes a plausible star profile by comparing the ratio of the big aperture and small aperture around the central star to a real star profile, namely the PSF. We see in table 3 the ratios and they are similar. This means we can use the mixed profile measurement as a replacement for the HD 100453 A measurement.

	I-band	R-band
PSF	0.58	0.49
Mixed Profile	0.62	0.51

Table 3: Ratio between the big and small aperture.

From the PSF ratio, we can also solve the problem of the big aperture measurement from ND4. Assuming we have similar ratios for the ND4 and the PSF, we can simply estimate the big aperture flux by dividing the small aperture flux by the ratio. We found a flux of  $1.34 \cdot 10^8$  for the I-band and  $2.33 \cdot 10^8$  for the R-band. This result is in good correspondence with the mixed profile value.



The mixed profile is not useful to measure the flux of the other objects considering it is a profile. But we can use cyc116 for that because, except for the saturation in HD 100453 A, it is a good observation. After following all the steps mentioned at the begging of this section. We can estimate the stellar magnitude of the objects in the cyc116 observation, see table 4.

	I-band		R-band	
	Ratio	Magnitude	Ratio	Magnitude
HD 100453 B	$4.70 \cdot 10^{-3}$	13.24 mag	$1.04 \cdot 10^{-3}$	15.06 mag
Distant Star	$1.65 \cdot 10^{-4}$	16.87 mag	$1.14 \cdot 10^{-4}$	17.45 mag
Ghost 1	$8.44 \cdot 10^{-5}$	17.60 mag	$6.15 \cdot 10^{-5}$	18.13 mag
Ghost 2	$2.03 \cdot 10^{-4}$	16.65 mag	$1.42 \cdot 10^{-4}$	17.22 mag

Table 4: The stellar magnitude of the objects and the ratio between the objects small aperture and the small aperture of the mixed profile.

### 3 Conclusion

We could make an estimate of the saturated peak of cyc116. This was done by fitting the profile of the ND4 observation to the profile of the cyc116 profile. It allowed us to measure the stellar magnitudes of the objects in cyc116. By measuring the flux in  $Q_\phi$  and in the constructed disk profile, we could determine that the disk of cyc116 has a reddish color.

A possible extension of the used methods, would be to try the fitting in 2 dimension.

### 4 References

- [1] Christian Tschudi. Dust cloud movement in r aquarii, 2018.
- [2] S. L. A. Vieira, W. J. B. Corradi, S. H. P. Alencar, L. T. S. Mendes, C. A. O. Torres, G. R. Quast, M. M. Guimares, and L. da Silva. Investigation of 131 herbig ae/be candidate stars. *The Astronomical Journal*, 126(6):2971–2987, dec 2003.

# Appendices

## A Photometric Data

### A.1 Big aperture data

Big Aperture	Counts w/o background			
	I-band		R-band	
	$I_Q$	$I_U$	$I_Q$	$I_U$
cyc116	$7.43 \cdot 10^7$	$7.58 \cdot 10^7$	$1.28 \cdot 10^8$	$1.32 \cdot 10^8$
ND4*	$3.85 \cdot 10^7$	$2.96 \cdot 10^7$	$3.19 \cdot 10^8$	$3.32 \cdot 10^8$
PSF	$4.08 \cdot 10^6$	$4.08 \cdot 10^6$	$6.89 \cdot 10^6$	$6.88 \cdot 10^6$
Mixed Profile	$1.34 \cdot 10^8$	$1.34 \cdot 10^8$	$2.12 \cdot 10^8$	$2.15 \cdot 10^8$

\* The counts of ND4 are not good for the big aperture because the observation is too faint.

Table 5: Calculated fluxes for the big aperture of radius 416px with an outer annulus radius of 466px. Different aperture sizes do not influence the flux by much. The difference between the  $I_Q$  and  $I_U$  should be seen as the measurement error.

### A.2 Small apertures data

Small Aperture	Counts w/o background**			
	I-band		R-band	
	$I_Q$	$I_U$	$I_Q$	$I_U$
HD 100453 A*	$2.40 \cdot 10^7 \pm 2\%$	$2.40 \cdot 10^7 \pm 2\%$	$2.57 \cdot 10^7 \pm 3\%$	$2.59 \cdot 10^7 \pm 3\%$
HD 100453 B	$3.98 \cdot 10^5 \pm 0.7\%$	$3.87 \cdot 10^5 \pm 0.7\%$	$1.16 \cdot 10^5 \pm 0.9\%$	$1.12 \cdot 10^5 \pm 0.9\%$
Distant Star	$1.42 \cdot 10^4 \pm 3\%$	$1.34 \cdot 10^4 \pm 3\%$	$1.26 \cdot 10^4 \pm 4\%$	$1.25 \cdot 10^4 \pm 4\%$
Ghost 1	$7.47 \cdot 10^3 \pm 0.7\%$	$6.61 \cdot 10^3 \pm 2\%$	$7.13 \cdot 10^3 \pm 4\%$	$6.35 \cdot 10^3 \pm 5\%$
Ghost 2	$1.91 \cdot 10^4 \pm 2\%$	$1.48 \cdot 10^4 \pm 4\%$	$1.91 \cdot 10^4 \pm 5\%$	$1.23 \cdot 10^4 \pm 6\%$
ND4	$7.74 \cdot 10^7 \pm 0.7\%$	$7.82 \cdot 10^7 \pm 0.7\%$	$1.13 \cdot 10^8 \pm 0.7\%$	$1.15 \cdot 10^8 \pm 0.7\%$
PSF	$2.39 \cdot 10^6 \pm 0.7\%$	$2.39 \cdot 10^6 \pm 0.7\%$	$3.35 \cdot 10^6 \pm 0.9\%$	$3.35 \cdot 10^6 \pm 0.8\%$
Mixed Profile	$8.40 \cdot 10^7 \pm 0.6\%$	$8.29 \cdot 10^7 \pm 0.5\%$	$1.10 \cdot 10^8 \pm 0.6\%$	$1.10 \cdot 10^8 \pm 0.6\%$
Disk	$Q_\phi: 4.22 \cdot 10^5$		$Q_\phi: 4.77 \cdot 10^5$	
cyc116 $Q$ -frame	$-4.70 \cdot 10^4 \pm 2\%$		$5.41 \cdot 10^4 \pm 5\%$	
cyc116 $U$ -frame	$4.53 \cdot 10^4 \pm 1\%$		$9.44 \cdot 10^4 \pm 2\%$	

\* The HD 100453 A is not correct because of the saturation.

\*\* For the calculation we used the mean of  $I_Q$  and  $I_U$ .

Table 6: Calculated fluxes for an aperture radius of 20px and annulus outer radius of 39px for the stars. The variation was calculated by moving the center of the aperture 1px in every direction as well as changing the radius by  $\pm 1$ , the standard deviation is then given as the percent value. For the disk an inner radius of 28px, a middle radius of 93px and an outer radius of 124px was chosen.

### A.3 Image of the small apertures

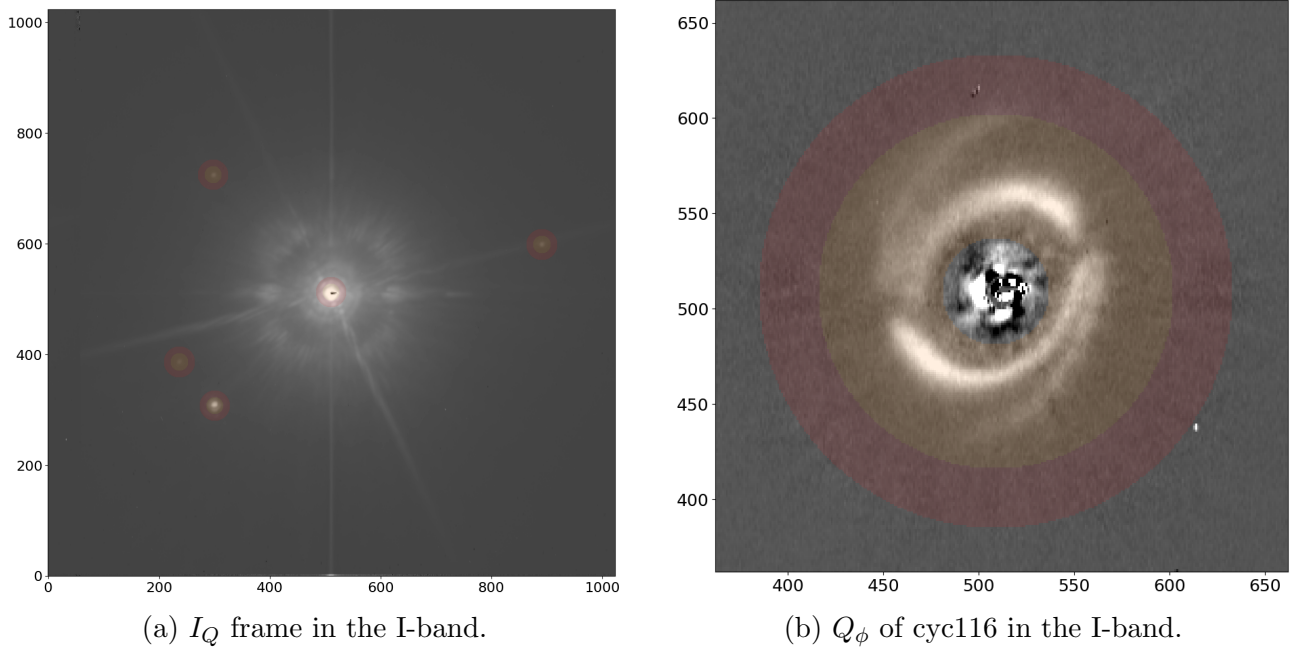


Fig. 9 cyc116 image of  $I_Q$  and  $Q_\phi$  with marked apertures.

### 4.4 Code

The code is available in the following GitHub repository: <https://github.com/ileu/SemesterWorks>